



This is a repository copy of *Global sensitivity analysis of a model for venous valve dynamics.*

White Rose Research Online URL for this paper:
<http://eprints.whiterose.ac.uk/103439/>

Version: Accepted Version

Article:

Keijsers, J.M., Leguy, C.A., Huberts, W. et al. (3 more authors) (2016) Global sensitivity analysis of a model for venous valve dynamics. *Journal of Biomechanics*. ISSN 0021-9290

<https://doi.org/10.1016/j.jbiomech.2016.06.029>

Reuse

This article is distributed under the terms of the Creative Commons Attribution-NonCommercial-NoDerivs (CC BY-NC-ND) licence. This licence only allows you to download this work and share it with others as long as you credit the authors, but you can't change the article in any way or use it commercially. More information and the full terms of the licence here: <https://creativecommons.org/licenses/>

Takedown

If you consider content in White Rose Research Online to be in breach of UK law, please notify us by emailing eprints@whiterose.ac.uk including the URL of the record and the reason for the withdrawal request.



eprints@whiterose.ac.uk
<https://eprints.whiterose.ac.uk/>

Global sensitivity analysis of a model for venous valve dynamics

J.M.T. Keijsers^{1,2,*}, C.A.D. Leguy², W. Huberts³, A.J. Narracott^{4,5}, J. Rittweger² and F.N. van de Vosse¹

¹ Department of Biomedical Engineering, Eindhoven University of Technology, Eindhoven, The Netherlands
² Institute of Aerospace Medicine, German Aerospace Center, Cologne, Germany ³ Department of Biomedical Engineering, Maastricht University, Maastricht, The Netherlands ⁴ Medical Physics Group, Department of Cardiovascular Science, University of Sheffield, Sheffield, United Kingdom ⁵ INSIGNEO Institute for *in silico* Medicine, University of Sheffield, Sheffield, United Kingdom

ABSTRACT

Chronic venous disease is defined as dysfunction of the venous system caused by incompetent venous valves with or without a proximal venous obstruction. Assessing the severity of the disease is challenging, since venous function is determined by various interacting hemodynamic factors. Mathematical models can relate these factors using physical laws and can thereby aid understanding of venous (patho-)physiology. To eventually use a mathematical model to support clinical decision making, first the model sensitivity needs to be determined. Therefore, the aim of this study is to assess the sensitivity of the venous valve model outputs to the relevant input parameters. Using a 1D pulse wave propagation model of the tibial vein including a venous valve, valve dynamics under head up tilt are simulated. A variance-based sensitivity analysis is performed based on generalized polynomial chaos expansion. Taking a global approach, individual parameter importance on the valve dynamics as well as importance of their interactions is determined. For the output related to opening state of the valve, the opening/closing pressure drop ($dp_{\text{valve},0}$) is found to be the most important parameter. The venous radius ($r_{\text{vein},0}$) is related to venous filling volume and is consequently most important for the output describing venous filling time. Finally, it is concluded that improved assessment of $r_{\text{vein},0}$ and $dp_{\text{valve},0}$ is most rewarding when simulating valve dynamics, as this results in the largest reduction in output uncertainty. In practice, this could be achieved using ultrasound imaging of the veins and fluid structure interaction simulations to characterize detailed valve dynamics, respectively.

Keywords: venous valves; versatile valve model; sensitivity analysis; chronic venous disease; generalized polynomial chaos expansion

Corresponding address: J.M.T. Keijsers, Department of Biomedical Engineering. Eindhoven University of Technology, PO Box 513, 5600 MB, Eindhoven. The Netherlands. Phone: +3140 247 5675. Email: j.m.t.keijsers@tue.nl

1 Introduction

Chronic venous disease is defined as dysfunction of the venous system caused by incompetent venous valves either with or without a proximal venous obstruction (international consensus committee on chronic venous disease (Porter et al. [1995])). As a result of venous valve incompetence, the muscle pump efficiency is significantly reduced, which has a negative effect on venous return, especially in upright position (Laughlin [1987]). Additionally, chronic venous disease results in increased venous pressure and blood accumulation in the leg (Bergan et al. [2006]). Venous hypertension, in turn, may contribute to the development of varicose veins (affecting one third of the Western population (Evans et al. [1999])) and in the long term to skin changes including pigmentation, venous eczema and even venous ulcers (chronic venous insufficiency) (Eberhardt and Raffetto [2005]).

For diagnosis of chronic venous disease Doppler ultrasound or phlebography (venous X-ray with contrast-agents) are often used to assess the location of leaking valves and varicose veins (Coleridge-Smith et al. [2006]; Eberhardt and Raffetto [2005]; Nicolaides [2000]). Although these methods can adequately detect local defects, they cannot determine the hemodynamic consequences of the disease, such as increased venous pressure and muscle pump inefficiency. Therefore, global measures such as venous pressure or venous calf volume (using air plethysmography (Criado et al. [1998]; Eberhardt and Raffetto [2005])) should be examined after calf muscle contractions or under head up tilt (i.e. going from supine to upright position without putting weight on the limb being measured). With these methods global diagnostic parameters, related to either venous refilling speed following tilt or ejection fraction after muscle contraction, can be assessed (Katz et al. [1991]); e.g. venous filling index ($VFI = \frac{\Delta V}{\Delta t} \Big|_{90\% \text{refilling}}$), which is measured after tilt. However, measuring venous pressure is invasive and air plethysmography is not available in every vascular laboratory.

An alternative approach to assess the global severity of chronic venous disease is the use of mathematical models based on physical laws and physiological mechanisms. These models can quantitatively predict hemodynamic parameters, that are important for the development of chronic venous disease and are difficult to measure. In the last decade, reduced order models of arterial hemodynamics have developed to a stage where they not only aid understanding cardiovascular (patho-)physiology (Boileau et al. [2015], Shi et al. [2011], van de Vosse and Stergiopoulos [2011]), but are also being validated to support clinical decision making (Caroli et al. [2013]; Marchandise et al. [2009]). For the venous system relatively few reduced order models have been developed to examine hemodynamics (Müller and Toro [2014]; Mynard and Smolich [2015]), regulation (Simakov et al. [2013]) and valve dynamics (Keijsers et al. [2015]), but these do include sufficient detail to capture generic venous function and the interplay between the various valves and veins. Although these models are suitable for assessment of the hemodynamic significance of chronic venous disease, they have not yet been applied in this context. Most models used to represent venous valve dynamics are generally only able to represent the open and closed state (diode) (Fullana and Zaleski [2008]; Müller and Toro [2014]; Zervides et al. [2008]), whereas reduced order heart valve models provide more detail (Werner et al. [2002]; Zacek and Krause [1996]). More sophisticated reduced-order valve models have been developed by Korakianitis and Shi [2006], who included valve leaflet motion based on a force balance and Mynard et al. [2012], who related valve opening state to the pressure drop over the valve. The latter model was extended by Pant et al. [2015] to include valve regurgitation due to valve prolapse. These versatile valve models are also preferred for the venous system as they can model regurgitation in leaking valves and allow more

detailed studies of venous valve dynamics, such as capturing venous valve dynamics under head up tilt. Unfortunately, these models require the introduction of more model parameters, which may increase the resulting uncertainty of the model output.

To eventually use such models to support clinical decision making, it is essential to assess the influence of the input parameters on the model output, which can be addressed through a sensitivity analysis. Using a global method both the importance of individual parameters and their interactions can be assessed (Eck et al. [2016]). Furthermore, knowing which parameters are most important, allows for refinement of clinical measurement protocols when using these models to support clinical decision making. Additionally, parameters that are difficult to measure can be assessed by using fluid structure interaction simulations.

The aim of this study is to investigate the sensitivity of a mathematical model of a tibial vein simulating venous valve dynamics under head up tilt. Our previously presented venous model (Keijsers et al. [2015]) is extended with the versatile valve model of Mynard et al. [2012]. The influence of venous filling and valve input parameters on the valve dynamics in a healthy subject is assessed via a sensitivity analysis based on generalized polynomial chaos expansion (gPCE). Finally, it is investigated whether more detailed fluid structure interaction simulations are necessary to inform the reduced order model.

2 Methods

To examine the dynamics of a healthy venous valve under head up tilt, a pulse wave propagation model of a vein including a single valve was developed (Figure 1). The pulse wave propagation model enables a continuous distribution of gravity, allows an easy extension of the model configuration to a larger domain and includes non-linear effects.

2.1 Model

The governing model equations are described in this section. This includes the 1D venous pulse wave propagation model, the 0D venous valve model and the boundary conditions. The baseline values of the model parameters can be found in Table 1.

Table 1: Model parameters: Baseline value and description are given. Furthermore, for the parameter included in the sensitivity analysis, the uncertainty range is given in the last column.

Symbol	Value	Unit	Description	Range
l_{dist}	10	<i>cm</i>	Length distal part 1D vein	-
l_{prox}	20	<i>cm</i>	Length proximal part 1D vein	-
p_{ex}	0	<i>Pa</i>	Extravascular pressure	-
g	9.81	$m \cdot s^{-2}$	Gravitational acceleration on earth	-
$A_{\text{eff,min}}$	$1 \cdot 10^{-20}$	m^2	Minimal effective cross-sectional area	-
α_{rot}	$0 - \pi/2$	<i>rad</i>	Tilting angle (supine to upright)	-
p_0	0	<i>Pa</i>	Extravascular pressure in windkessel element	-
$p_{\text{wk,in}}$	12.0	<i>kPa</i>	Constant inlet pressure	-
$p_{\text{wk,out}}$	700	<i>Pa</i>	Constant outlet pressure	-
η	$4.5 \cdot 10^{-3}$	<i>Pa</i>	Dynamic blood viscosity: Typical viscosity used in 1D hemodynamics models is taken as a reference with an uncertainty of 20% (Boileau et al. [2015]).	$[3.6, 5.4] \cdot 10^{-3}$

Table 1 – continued from previous page

Symbol	Value	Unit	Description	Range
β_l	1.0	-	Effective length venous valve ratio ($\beta_l = \frac{l_{\text{eff}}}{r_{\text{vein},0}}$): Ratio of the effective length of the venous valve relative to the radius of the connecting vein (Mynard and Smolich [2015])	[0.5, 2.0]
ρ	1050	kg/m^3	The arterial blood density has a value between the 1045 and 1055 kg/m^3 and venous blood density is on average 0.1 kg/m^3 less than arterial blood density (Kenner [1989]).	[1040, 1060]
β_A	0.65	-	Effective valve cross-sectional area ratio $\beta_A = \frac{A_{\text{eff,max}}}{A_{\text{vein},0}}$: Ratio of valve cross-sectional area to the cross-sectional area of the connecting vein. The valve is observed to create a stenosis in the fully open state (Lurie et al. [2003]; McCaughan et al. [1984]).	[0.4, 1.0]
K_{vo}	0.3	$Pa^{-1} \cdot s^{-1}$	Valve opening constant: The full range of values reported by Mynard and Smolich [2015] is covered.	[0.2, 0.4]
K_{vc}	0.3	$Pa^{-1} \cdot s^{-1}$	Valve closing constant: The full range of values reported by Mynard and Smolich [2015] is covered.	[0.2, 0.4]
$dp_{\text{valve},0}$	0	Pa	Opening/closing pressure drop over the valve ($dp_{\text{valve},0} = p_{\text{dist}} - p_{\text{prox}}$) (Figure 3C): Pressure drop over the valve above and below which valve opening and closing are initiated, respectively. This pressure drop is assumed to be close to zero (Mynard et al. [2012]).	[-10, 10]
q_{bl}	0.45	mL/s	Baseline flow: The flow is defined to represent the flow in the tibial vein with an uncertainty of 10% (Saltin et al. [1998]).	[0.405, 0.495]
K_p	425	Pa	Venous bending stiffness: The bending stiffness is defined to represent the mechanical characteristics of the tibial vein with an uncertainty of 20% (Müller and Toro [2014]).	[340, 510]
$r_{\text{vein},0}$	1.50	mm	Radius of the 1D vein: The radius is defined as the radius of the tibial vein with an uncertainty of 20% (Müller and Toro [2014]).	[1.20, 1.80]
τ_{RC}	2.0	s	Time constant defining the decay of the pressure wave in diastole: Most of the compliance is included in the WK-element (Westerhof and Elzinga [1991]). Uncertainty is set to 20%.	[1.6, 2.4]

1D Venous pulse wave propagation

The hemodynamics in the large veins are captured using the one-dimensional equations for mass and momentum balance. In this formulation, blood is assumed to be an incompressible, Newtonian fluid. This gives:

$$C \frac{\partial p_{tr}}{\partial t} + \frac{\partial q}{\partial z} = 0, \quad (1)$$

$$\frac{\partial q}{\partial t} + \frac{\partial A \bar{v}_z^2}{\partial z} + \frac{A}{\rho} \frac{\partial p}{\partial z} = \frac{2\pi a}{\rho} \tau_w + A g_z, \quad (2)$$

where C , compliance per unit length, is a function of transmural pressure $p_{tr} = p - p_{ex}$, where p and p_{ex} are the intra- and extravascular pressure respectively, q is flow, t is time and z is the axial coordinate. Furthermore, A is the cross-sectional area, \bar{v}_z is the mean velocity in the axial direction, ρ is the blood density, $a = \sqrt{A/\pi}$ is the equivalent radius for equal area, τ_w is the wall shear stress and $g_z = g \mathbf{e}_g \cdot \mathbf{e}_z$ is the contribution of gravitational acceleration in the axial direction. Additionally, g is the gravitational acceleration

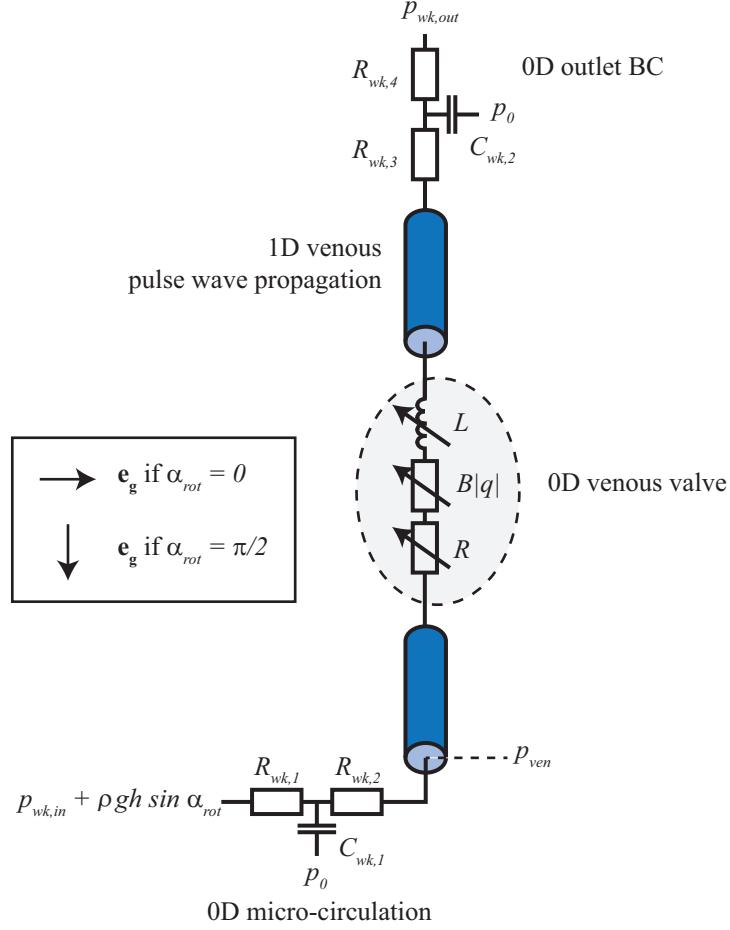


Figure 1: Model configuration consisting of a 0D venous valve, 1D venous pulse wave propagation elements, a 0D micro-circulation and a 0D outlet boundary condition (BC). Furthermore, the gravity vector \mathbf{e}_g is shown together with the rotation angle in both supine and tilted position. The 1D vein is split into a distal ($l_{\text{dist}} = 10 \text{ cm}$) and a proximal ($l_{\text{prox}} = 20 \text{ cm}$) part by a 0D valve (zero length). p_{ven} indicates the location of distal venous pressure as reported in the Results Section in Figure 4E.

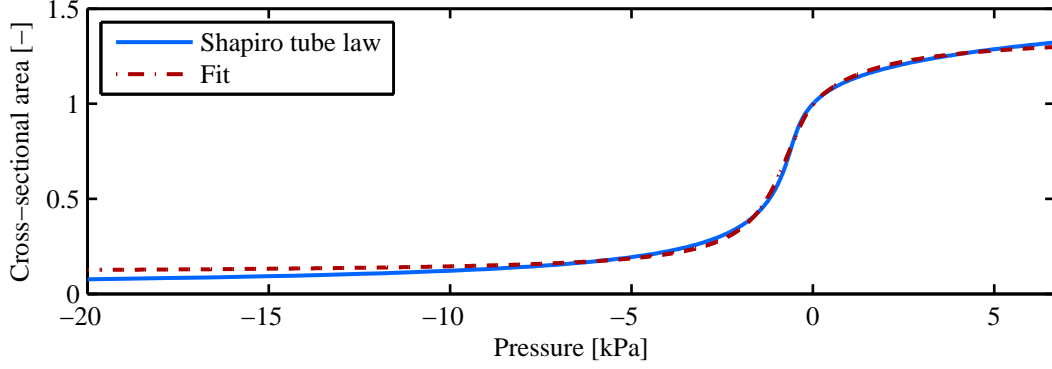


Figure 2: A, p -relation according to Shapiro tube law: Shapiro et al. (-) and the fit of Keijsers et al. [2015]. Figure copied from Keijsers et al. [2015]

on earth, \mathbf{e}_g is the unit vector in the direction of gravity and \mathbf{e}_z is the unit vector in the axial direction along the vessel.

To obtain an estimate of the wall shear stress τ_w and the advection term $\frac{\partial A \bar{v}_z^2}{\partial z}$ the approximate velocity profile of Bessems et al. [2007] is used. The pressure gradient and gravitational forces are assumed to be in balance with viscous forces in the unsteady boundary layer (Stokes layer) close to the vessel wall, whereas inertia forces are assumed to dominate in the central core (for a detailed description see Bessems et al. [2007]).

To describe venous collapse under low transmural pressure, due to e.g. increasing extravascular pressure or gravitational stress, the non-linear constitutive law of Shapiro [1977] is approximated with a fit, which we presented in a previous study (Keijsers et al. [2015]) (Figure 2). The venous compliance per unit length C is calculated as the derivative of the cross-sectional area to the transmural pressure.

0D Venous valve

The pressure-flow relation of a dynamic venous valve is included through a fully lumped model (i.e. the valve element has no length and spatial parameters are only included for dimensionality) as described by Mynard et al. [2012]. Additionally, the viscous losses are included in the pressure flow relation

$$\Delta p = Rq + Bq|q| + L \frac{\partial q}{\partial t}, \quad (3)$$

where Rq represent the viscous losses, $Bq|q|$ the losses related to the convective acceleration and dynamic pressure, and $L \frac{\partial q}{\partial t}$ the unsteady inertia losses. The associated Poiseuille resistance R , Bernouilli resistance B and inertia L are defined by:

$$R = \frac{8\pi\eta l_{\text{eff}}}{A_{\text{eff}}^2}, \quad B = \frac{\rho}{2A_{\text{eff}}^2} \quad \text{and} \quad L = \frac{\rho l_{\text{eff}}}{A_{\text{eff}}}, \quad (4)$$

where A_{eff} is the effective cross-sectional area, ρ is the blood density and $l_{\text{eff}} = \beta_l r_{\text{vein},0}$ is the effective valve length expressed as a multiple β_l of the reference radius of the connecting vein $r_{\text{vein},0}$. To represent different states of the valve opening the effective cross-sectional area is defined as a function of valve state ζ via the following relation

$$A_{\text{eff}} = (A_{\text{eff,max}} - A_{\text{eff,min}}) \zeta + A_{\text{eff,min}}, \quad (5)$$

where $A_{\text{eff,min}}$ and $A_{\text{eff,max}}$ are the minimal and maximal valve effective cross-sectional area respectively ($A_{\text{eff,max}} \gg A_{\text{eff,min}}$). $A_{\text{eff,max}} = \beta_A A_{\text{vein},0}$ is expressed as a multiple β_A

of the reference cross-sectional area of the connecting vein $A_{\text{vein},0}$. To model a dynamic valve, the valve state is defined to vary between zero and one (closed: $\zeta = 0$, open: $\zeta = 1$). The value of ζ is determined by the differential equations for valve opening and closing respectively

$$\frac{d\zeta}{dt} = \begin{cases} (1 - \zeta) K_{\text{vo}} (\Delta p - dp_{\text{valve},0}), & \text{for } \Delta p > dp_{\text{valve},0} \\ \zeta K_{\text{vc}} (\Delta p - dp_{\text{valve},0}), & \text{for } \Delta p < dp_{\text{valve},0} \end{cases}, \quad (6)$$

where K_{vo} and K_{vc} are parameters determining the opening and closing speed of the valves. Furthermore, $dp_{\text{valve},0}$ is the pressure gradient above and below which opening and closing is initiated respectively.

Boundary conditions

Both the inlet and outlet of the modeled vein are connected to a three-element windkessel model, representing the micro-circulation at the inlet and included to reduce reflections at the outlet (Figure 1). Each windkessel model consists of two resistances $R_{\text{wk},i}$ ($i = 1, 2, 3, 4$) in series and one volume compliance $C_{\text{wk},j}$ ($j = 1, 2$) connected to a constant extravascular pressure p_0

$$\Delta p_R = R_{\text{wk},i} q \quad \text{and} \quad \frac{\partial p_{\text{tr}}}{\partial t} = \frac{1}{C_{\text{wk}}} q. \quad (7)$$

For the windkessel element at the inlet the second resistance is defined to match the characteristic impedance Z_{vein} of the connecting 1D vein

$$R_{\text{wk},1} = Z_{\text{vein}} = \sqrt{\frac{\rho}{A_{\text{vein},0} C_{\text{vein},0}}}. \quad (8)$$

The first resistance is related to the total windkessel resistance $R_{\text{wk,tot}}$ which is set to match the baseline flow q_{bl}

$$R_{\text{wk,tot}} = R_{\text{wk},1} + R_{\text{wk},2} = \frac{\Delta p}{q_{\text{bl}}}, \quad (9)$$

where Δp is the gradient between inlet pressure $p_{\text{wk,in}}$ and the distal venous pressure under supine baseline conditions. The latter is derived as the outlet pressure p_{out} plus the baseline flow q_{bl} times the resistance of the 1D vein and outlet windkessel element. Next, the compliance is derived from a time constant τ_{RC}

$$C_{\text{wk},1} = \frac{\tau_{\text{RC}}}{R_{\text{wk},2}}. \quad (10)$$

For the windkessel element at the outlet, both resistances are defined to be equal to the characteristic impedance Z_{vein} of the connecting vein

$$R_{\text{wk},3} = R_{\text{wk},4} = Z_{\text{vein}} = \sqrt{\frac{\rho}{A_{\text{vein},0} C_{\text{vein},0}}}. \quad (11)$$

The outlet compliance $C_{\text{wk},2}$ is derived from the time constant τ_{RC} using Equation 10.

In the current model pressure is prescribed as a boundary condition and flow is only indirectly prescribed by defining the resistance of the micro-circulation. The outlet pressure p_{out} is defined to have a constant value and the inlet pressure is defined as p_{in} a constant value plus the hydrostatic column of the 1D part.

$$p_{\text{in}} = p_{\text{wk,in}} + \rho g h \sin \alpha_{\text{rot}} \quad \text{and} \quad p_{\text{out}} = p_{\text{wk,out}}, \quad (12)$$

where $p_{wk,in}$ is the average arterial pressure, h is the total length of the 1D vein, α_{rot} is the rotation angle determining the posture and $p_{wk,out}$ is a constant pressure at the outlet.

Numerical implementation

The equations detailed above were implemented in the finite element package SEPRAN (Ingenieursbureau SEPRA, Leidschendam, the Netherlands) based on the computational method described by Kroon et al. [2012]. Spatial discretization was implemented using the trapezium rule with element size $dz = 10 \text{ mm}$. Time discretization was performed using the second-order backward difference scheme with timestep $dt = 10 \text{ ms}$. Both dz and dt were chosen such that the numerical solution was independent of the selected values and still computationally efficient. Further pre- and postprocessing was done using MATLAB R2012b (MathWorks, Natick, MA, USA).

2.2 Head up tilt simulation

A head up tilt was simulated to study the opening and closing of the valve under gravitational stress. To simulate a smooth head up tilt from supine ($\alpha_{rot} = 0$) to upright ($\alpha_{rot} = \frac{\pi}{2}$) the tilt angle α_{rot} was defined with the following relation (Figure 4A):

$$\alpha_{rot} = \begin{cases} 0, & \text{if } t < t_0 \\ \frac{\pi}{4} (1 - \cos(\pi(t - t_0)/\tau_{rot})), & \text{if } t_0 < t < t_0 + \tau_{rot} \\ \frac{\pi}{2}, & \text{if } t > t_0 + \tau_{rot}. \end{cases} \quad (13)$$

where t_0 is the time at which the tilt starts and τ_{rot} is the time over which the tilt is applied. The latter is set to 2.5 s to correspond with *in vivo* experiments (Jellema et al. [1999]).

2.3 Sensitivity analysis

To determine the importance of the model parameters, first the output variance resulting from the input uncertainty was quantified. Using a sensitivity analysis, the total variance of each output was then allocated to the individual parameters and their interactions, as schematically visualized in Figure 3A. The influence of an individual parameter is captured by the main sensitivity index S_i , and can be interpreted as the reduction in output variance if this input parameter would have been set to its true value. Higher order effects (S_{ij} , S_{ijk} , ...) include the contribution between interactions of two or more input parameters (Eck et al. [2016]).

Output of interest

The following parameters, which describe valve dynamics, are defined as output of interest (Figure 3B):

- ζ_{bl} , baseline valve state (not necessarily equal to 1.0).
- t_c , time point valve closure starts: the first time point after tilt when the valve state decreases below $0.95\zeta_{bl}$.
- dt_c , valve closing time: the time taken to go from 0.95 to $0.05\zeta_{bl}$.
- dt_{fc} , valve fully closed time: the interval between the time the valve state first decreases below $0.05\zeta_{bl}$ until it increases above $0.05\zeta_{bl}$.
- dt_o , valve opening time: the time taken to go from 0.05 to $0.95\zeta_{bl}$.

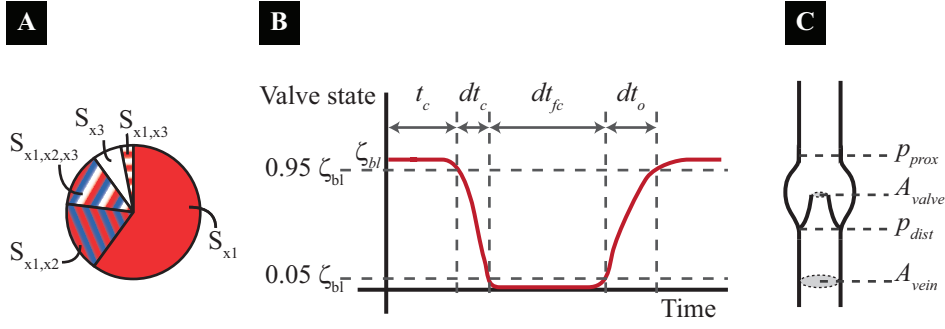


Figure 3: Sensitivity analysis: **A** Schematic visualisation of the distribution of the output variance over the input parameters: x_1 , x_2 and x_3 . S_i = main index, S_{ij} = second order effect, S_{ijk} = third order effect. **B** Output parameters of interest schematically visualized in a plot of the valve state ζ over time. **C** Parameters related to the input parameters used in the sensitivity analysis, visualized in a segment of a vein including a valve.

General polynomial chaos expansion

To derive the total variance and the sensitivity indices in a computationally efficient manner, the generalized polynomial chaos expansion (gPCE-R) method is used (Huberts et al. [2014]). This includes the derivation of a meta-model consisting of orthogonal polynomials with output-specific coefficients, which are obtained by a least-squares regression (-R). The sensitivity indices can be derived from the meta-model analytically. To obtain a good regression for the chosen meta-model, the model must be evaluated a sufficient number of times. In this study, the meta-model consists of orthogonal polynomials up to the fourth order and 2730 model evaluations ($CPU \approx 15 h$) are used for regression.

Input parameters

The sensitivity of the model with regard to the valve dynamics is examined under variation of the 11 input parameters related to venous valve dynamics and venous refilling. These parameters are listed in Table 1, which provides the baseline value and the range used for the sensitivity analysis.

3 Results

3.1 Venous valve dynamics

The valve dynamics and venous hemodynamics were examined while simulating a head up tilt (Figure 4A) in a 1D venous model with a single 0D valve. With all input parameters fixed at their baseline value, the resulting valve state ζ , valve pressure drop Δp_{valve} , valve flow q_{valve} , venous pressure and total volume are shown in Figure 4B, C, D, E and F respectively. Shortly after tilt is initiated, the valve flow decreases (Figure 4D) and the valve closes (Figure 4B). This is followed by a decrease in pressure difference across the valve (Figure 4C). The venous pressure and total volume increase linearly ($VFI = \frac{\Delta V}{\Delta t} \Big|_{90\% \text{ refilling}} = 0.5 \text{ mL/s}$ Figure 4E and F respectively) until the pressure drop over the valve approaches zero, the valve starts to open and the flow increases again at $t \approx 15.7 \text{ s}$ (Figure 4C, B and D respectively).

3.2 Convergence analysis

To assess the quality of the metamodel the descriptive error ϵ_{R^2} , a measure for the residual variance as a fraction of total variance and based on the coefficient of determination

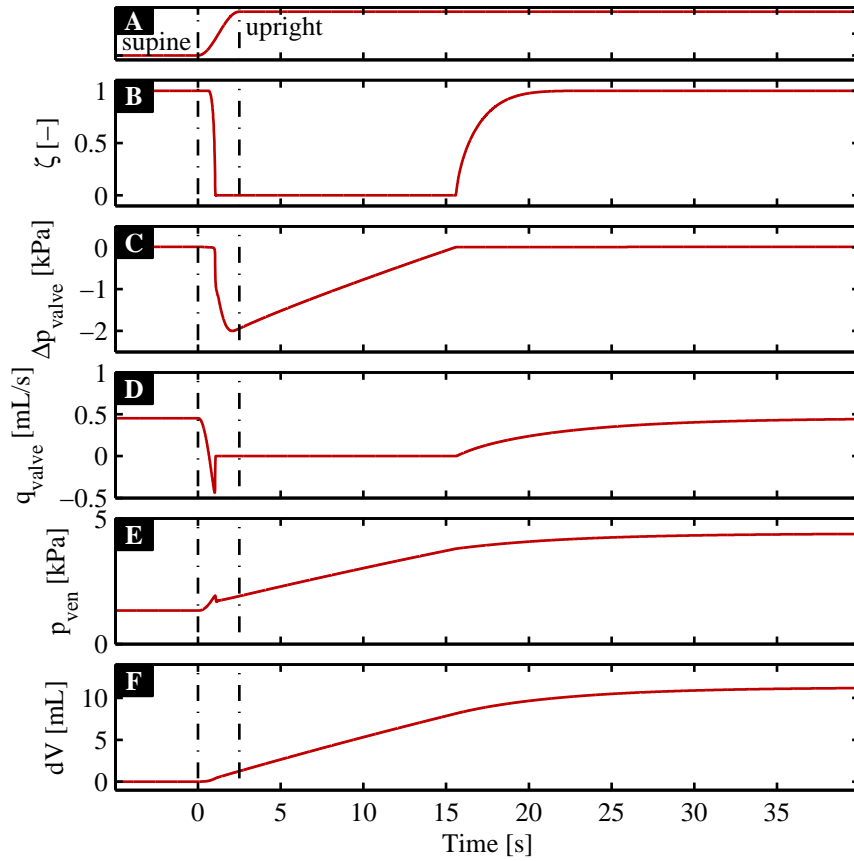


Figure 4: Valve dynamics and hemodynamics under head up tilt for baseline input parameters (Table 1 - Input parameters). In plot **A** the time course of the tilt is shown. The beginning and end of the tilt are indicated with a dashed line in each plot. Plot **B**, **C** and **D** show the state ζ , pressure drop Δp_{valve} and flow q_{valve} of the valve respectively. Distal venous pressure p_{ven} (as indicated in Figure 1) and change in total volume (the sum of the 0D micro-circulation and the 1D vein) are shown in plot **E** and **F** respectively.

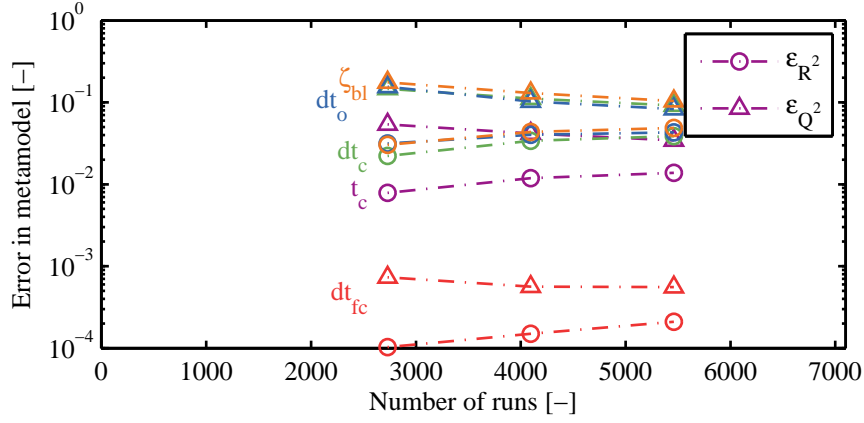


Figure 5: The quality of the metamodel for each output parameter. The descriptive error ϵ_{R^2} (o) and the predictive error ϵ_{Q^2} (Δ) are plotted for increasing number of simulations. The colors represent the different output parameters: t_c (purple), dt_c (green), dt_{fc} (red), dt_o (blue) and ζ_{bl} (orange).

R^2 , and the predictive error ϵ_{Q^2} , a measure for the predicted residual variance as a fraction of total variance and based on the validation coefficient Q^2 , were calculated for an increasing number of simulations (Donders et al. [2015]) (o and Δ in Figure 5 respectively). The different output parameters are depicted with different colors. Both the descriptive and predictive errors remain stable for increasing number of simulations.

3.3 Sensitivity analysis

The contribution of the valve and refilling related input parameters to the variance in valve timings was assessed using a sensitivity analysis. The resulting main (S_i) and interaction (S_{ij} , S_{ijk} , S_{ijkl}) sensitivity indices are presented in pie charts in Figure 6. The input parameters which, individually or while interacting with other parameters, contribute more than 1% to the output variance are presented with their corresponding color, whereas the sum of the remaining sensitivity indices is shown as the gray area (■). The values of the sensitivity indices presented in Figure 6 are summarized in Table 2. For t_c , dt_c , dt_o and to a lesser extent ζ_{bl} the pressure drop for valve opening and closing $dp_{valve,0}$ is the input parameter which contributes the most to the output variance (■ in Figure 6A,B,D and E respectively). The venous radius $r_{vein,0}$ is the most important parameter for the variance of dt_{fc} (■ Figure 6C). The interaction of various parameters contributes to the variance of t_c , dt_c , dt_o and especially ζ_{bl} (Figure 6B). The interactions of $dp_{valve,0}$ with β_A and/or $r_{vein,0}$ are shown to be important for ζ_{bl} (Figure 6E).

The average values of the output parameters plus their standard deviations are shown in Figure 7 depicting the absolute and relative values in plot A and B, respectively. Here, the relative value is calculated using: $y_{rel} = \frac{y_i - y_{mean}}{y_{mean}}$. A large standard deviation is found for dt_{fc} and dt_o . Although the absolute standard deviation is small, the relative standard deviation is large for t_c and dt_c .

The relation between the input parameters with the highest main sensitivity index ($dp_{valve,0}$ and $r_{vein,0}$) and the output parameters is presented in Figure 8. The output and input parameters are shown by row and column respectively. Furthermore, the gray scale is related to the magnitude of the main sensitivity index S_i (see colorbar). The time of closing t_c decreases with an increasing pressure drop for valve opening and closing $dp_{valve,0}$ (Figure 8A), whereas the time needed for the valve to open and close increases with $dp_{valve,0}$

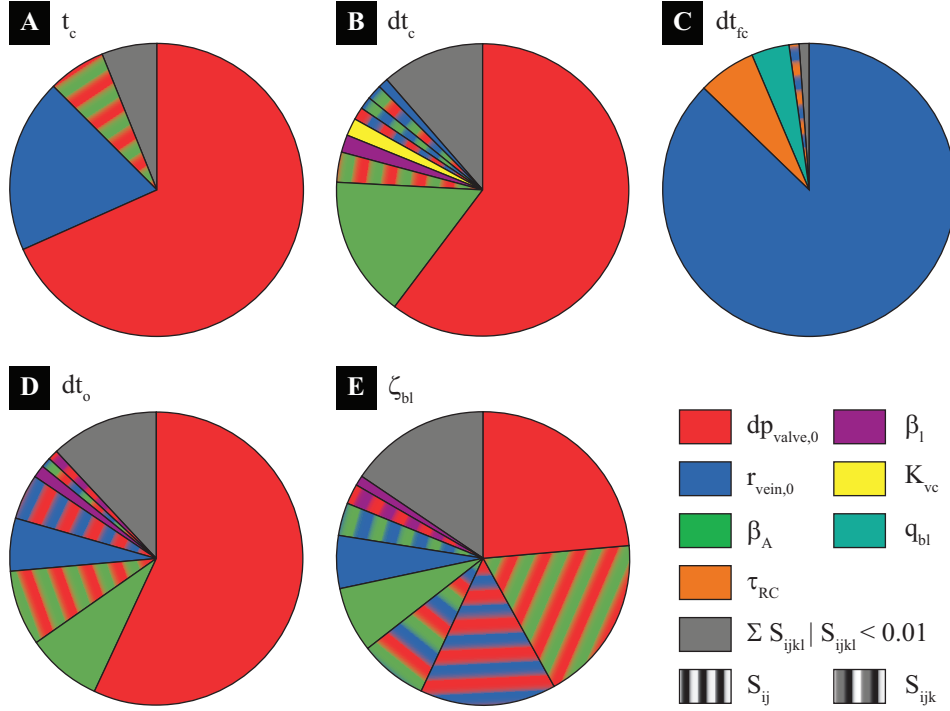


Figure 6: Contribution of the input parameters to the variance in the output parameters: **A** t_c , **B** dt_c , **C** dt_{fc} , **D** dt_o and **E** ζ_{bl} . The colors represent the various input parameters contributing more than one percent to the output variance. Second and third order interactions (S_{ij} and S_{ijk}) are presented with a combination of the colors. The gray area (■) represents the sum of the sensitivity indices which individually contribute less than one percent. The size of the sensitivity index decreases clockwise starting at noon position. The values of the sensitivity indices can be found in Table 2. See pdf for the color version.

Table 2: Contribution of the input parameters to the variance in the output parameters: t_c , dt_c , dt_{fc} , dt_o and ζ_{bl} . Only the sensitivity indices that contribute more than one percent are reported in the table. Coloring corresponds to the coloring used for the pie-charts in Figure 6

	t_c	dt_c	dt_{fc}	dt_o	ζ_{bl}
$dp_{valve,0}$ (■)	0.683	0.601	< 0.01	0.572	0.237
$r_{vein,0}$ (■)	0.194	0.012	0.874	0.058	0.060
β_A (■)	< 0.01	0.154	< 0.01	0.084	0.072
τ_{RC} (■)	< 0.01	< 0.01	0.063	< 0.01	< 0.01
β_l (■)	< 0.01	0.020	< 0.01	0.013	0.0011
K_{vc} (■)	< 0.01	0.018	< 0.01	< 0.01	< 0.01
q_{bl} (■)	< 0.01	< 0.01	0.044	< 0.01	< 0.01
$dp_{valve,0}, r_{vein,0}$ (■)	< 0.01	0.015	< 0.01	0.051	0.150
$dp_{valve,0}, \beta_A$ (■)	0.063	0.039	< 0.01	0.082	0.183
$dp_{valve,0}, \beta_l$ (■)	< 0.01	< 0.01	< 0.01	0.012	0.023
$r_{vein,0}, \beta_A$ (■)	< 0.01	0.015	< 0.01	< 0.01	0.035
$r_{vein,0}, \tau_{RC}$ (■)	< 0.01	< 0.01	0.011	< 0.01	< 0.01
$dp_{valve,0}, r_{vein,0}, \beta_A$ (■)	< 0.01	0.015	< 0.01	0.012	0.075
rest (■)	0.060	0.112	0.008	0.118	0.154

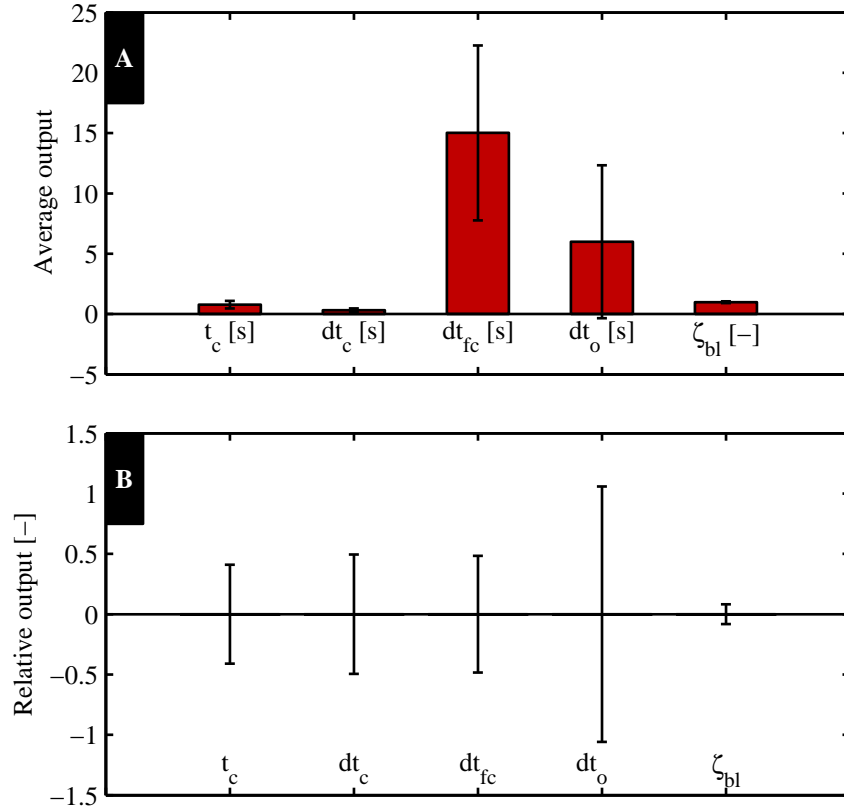


Figure 7: Average and standard deviation of the output parameters: **A** absolute and **B** relative value.

(Figure 8C,G). The $r_{vein,0}$ parameter shows a strong linear relation with dt_{fc} (99% of S_i is attributed to the first order polynomial) (Figure 8F). The remaining plots (Figure 8B, D, E, H, I and J) show a lower correlation and have a lower sensitivity index.

4 Discussion

In this study the venous valve dynamics in a healthy subject under head up tilt was investigated using a mathematical model of a single vein geometry including a single versatile valve. To assess the influence of the various filling and valve input parameters on valve dynamics, a sensitivity analysis was performed.

A head up tilt was simulated by rotating a single vein relative to the gravity vector (using baseline parameters). Shortly after tilt initiates, a decrease in valve flow was observed and even some backflow for 0.4 s. This corresponds to the non-pathological range ($dt_{reflux} < 0.5$ s) according to the definition of venous reflux in the deep calf veins by Labropoulos et al. [2003]. Once tilting was initiated the vein and micro-circulation started to fill to approach the hydrostatic pressure. The observed linear-plateau pressure and volume pattern is in accordance with *in vivo* measurements after muscle contractions (Nicolaidis and Zukowski [1986]), where the veins are also refilled. As only a small part of the vasculature is included the hydrostatic pressure is smaller than the 12 kPa measured *in vivo*, but does match the physically expected $\rho gh = 3.1$ kPa. This small increase in venous pressure (from 1.3 to 4.4 kPa) induces only a small increase in 1D volume (1.3% of total) (see Figure 2). Venous filling index (VFI), a measure of venous filling speed, is equal to 0.5 mL/s, which is in the region of VFI for healthy subjects ($VFI < 2.0$ mL/s)

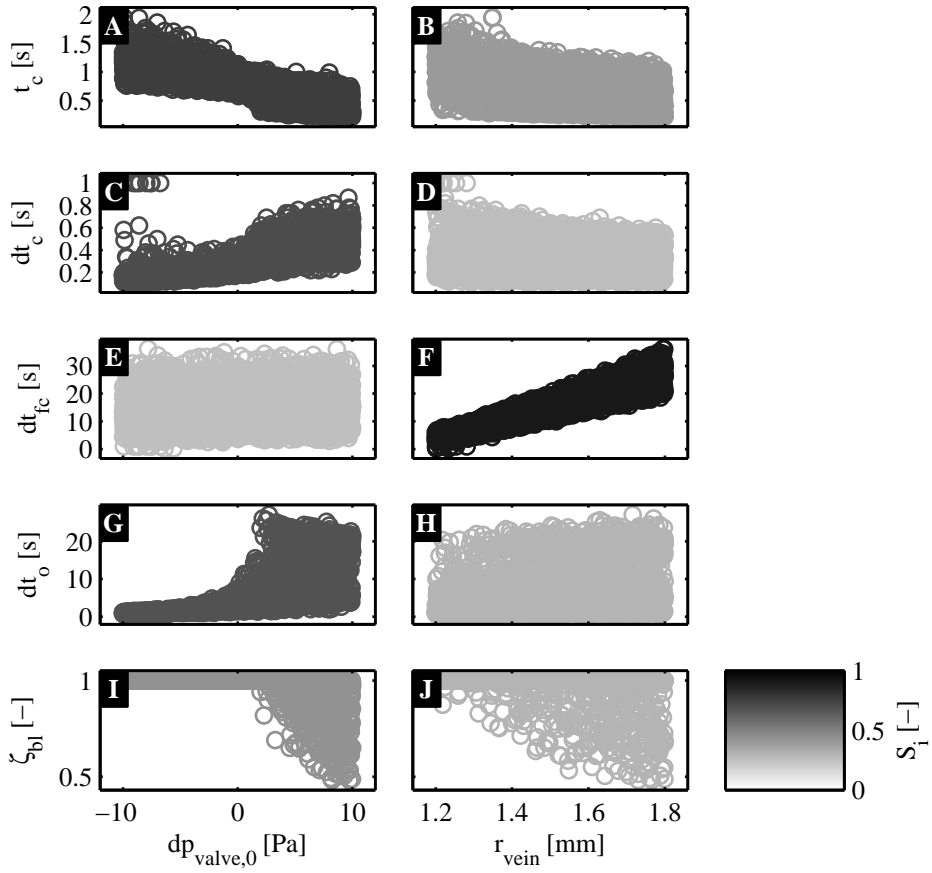


Figure 8: The relation between the two dominating input parameters ($dp_{\text{valve},0}$ (left) and $r_{\text{vein},0}$ (right)) and all the output parameters is presented with scatter plots, where each circle represents a single simulation. The output parameters are shown by row and the input parameters by column; the first row presents the relation between output t_c and input $dp_{\text{valve},0}$ on the left (A), and input $r_{\text{vein},0}$ on the right (B). The rest of the output parameters are presented similarly in the subsequent rows. The gray scale represents the main sensitivity index S_i , with darker gray for the higher values as indicated with the colorbar. The values of the main sensitivity indices can be found in the first two rows of Table 2.

(Eberhardt and Raffetto [2005]). In short, this implies that the observed pressure and volume pattern and derived global hemodynamics parameters are in accordance with the literature.

The sensitivity analysis showed that $dp_{\text{valve},0}$, $r_{\text{vein},0}$ and β_A are the most influential parameters with more than 80% of the variance of all output parameters arising from the sum of the individual and interactive contributions of these three parameters, i.e. $S_i + S_{ij} + S_{ijk}$. The valve opening pressure $dp_{\text{valve},0}$ is closely related to the opening and closing of the valve and therefore the observed importance of this parameter on output parameters related to valve state (t_c , dt_c , dt_o and ζ_{bl}) is also expected. The venous reference radius $r_{\text{vein},0}$ is related to venous filling volume and is consequently the most important parameter for the output describing venous filling time dt_{fc} . Finally, β_A is related to the valve resistance in the open state and is therefore important for the valve dynamic output parameters (dt_c , dt_o and ζ_{bl}). All other parameters only have a minor contribution to the output variance and can therefore be fixed within their uncertainty range. In order to use the model for clinical decision making, the output variance should be decreased. For this, ultrasound could be used to assess β_A (Lurie et al. [2003]) and $r_{\text{vein},0}$ (Moneta et al. [1988]) and further research using fluid-structure interaction simulations could decrease the uncertainty range of $dp_{\text{valve},0}$ (Narracott et al. [2015]). Improved assessment of $r_{\text{vein},0}$ and $dp_{\text{valve},0}$ would be most rewarding as the standard deviation of dt_{fc} and dt_o respectively is the largest. When the output parameters are considered in the context of chronic venous disease estimates of $r_{\text{vein},0}$ should be improved as dt_{fc} provides a metric of venous filling time, which is related to venous function.

The sensitivity indices were derived using the generalized polynomial chaos expansion method. The quality of the metamodel was assessed by the descriptive and predictive error (Donders et al. [2015]). While deriving the metamodel for an increasing number of simulations, a slight increase in the descriptive error of the model (ϵ_{R^2}), and an increase in predictive power (decrease in ϵ_{Q^2}) was found. The convergence analysis demonstrated that only 5% of the output variance could not be captured by the metamodel (ϵ_{R^2} in Figure 5). Thereby, showing that the gPCE methods provides significant accuracy for this application.

The current paper describes the feasibility of applying the versatile valve model and the venous 1D pulse wave propagation model in supporting diagnosis of chronic venous disease. Further development should allow for modeling of pathological valve regurgitation, which Mynard et al. [2012] suggested to implement by an increase in minimal cross-sectional area A_{min} resulting in a valve model that remains partially open. Valve prolapse could be included by defining a negative valve state, as suggested by Pant et al. [2015]. Furthermore, as chronic venous disease affects the global function of the venous calf circulation, the full venous calf geometry should be incorporated to include interactions between the many valves and the complex venous anatomy, which is possible using the 1D pulse wave propagation model as proposed in our previous study (Keijsers et al. [2015]). Additionally, as venous refilling is achieved when the full hydrostatic pressure is established, the proximal veins returning to the heart should also be included. A full circulation model would also allow examination of the influence of venous pulsatility, originating from the thorax and abdomen, on the venous valves. Finally, the model should be validated with fluid-structure interaction simulations or *in vivo* measured hemodynamics parameters such as the venous filling index after tilt or ejection fraction after muscle contraction (Eberhardt and Raffetto [2005]; Criado et al. [1998]).

5 Conclusion

A venous 1D pulse wave propagation model including a versatile valve model is presented and a sensitivity analysis has been performed on the model while capturing venous valve dynamics in a healthy subject under head up tilt. It has been shown that venous radius $r_{\text{vein},0}$ and valve opening/closing pressure $dp_{\text{valve},0}$ are the dominant parameters, which determine the variance in valve dynamics. Decreasing the uncertainty in these parameters to improve the model output accuracy could be achieved by improving clinical assessment via ultrasound or informed by more detailed mathematical models using fluid structure interaction. This would support eventual implementation of the model in clinical practice to aid clinical decision making.

Acknowledgements

We gratefully acknowledge W.P. Donders for his assistance and providing the framework for the sensitivity analysis. J.M.T. Keijsers received a scholarship of the Helmholtz SpaceLife Sciences Research School (SpaceLife) which was funded by the Helmholtz Association and the German Aerospace Center (Deutsches Zentrum für Luft- und Raumfahrt e.V., DLR). The contribution of Dr. A.J. Narracott to this research was supported by funding from the Research Mobility Programme of the Worldwide Universities Network. The contribution of Dr. C.A.D Leguy was performed with the support of the Marie Curie International Outgoing fellowship of the European's 7th Framework Programme for Research under contract number MC-IOF-297967.

Disclosures

No conflicts of interest are declared by the authors.

References

- J. J. Bergan, G. W. Schmid-Schönbein, P. D. Coleridge Smith, A. N. Nicolaidis, M. R. Boisseau, and B. Eklof. Chronic venous disease. *N Engl J Med*, 355(5):488–498, 2006.
- D. Bessems, M. Rutten, and F. Van De Vosse. A wave propagation model of blood flow in large vessels using an approximate velocity profile function. *J Fluid Mech*, 580:145–168, 2007.
- E. Boileau, P. Nithiarasu, P. J. Blanco, L. O. Mueller, F. E. Fossan, L. R. Hellevik, W. P. Donders, W. Huberts, M. Willemet, and J. Alastruey. A benchmark study of numerical schemes for one-dimensional arterial blood flow modelling. *Int J Numer Method Biomed Eng*, 31(10):e02732, 2015.
- A. Caroli, S. Manini, L. Antiga, K. Passera, B. Ene-Iordache, S. Rota, G. Remuzzi, A. Bode, J. Leermakers, F. N. van de Vosse, R. Vanholder, M. Malovrh, J. Tordoir, and A. Remuzzi. Validation of a patient-specific hemodynamic computational model for surgical planning of vascular access in hemodialysis patients. *Kidney Int*, 84(6):1237–1245, 2013.
- P. Coleridge-Smith, N. Labropoulos, H. Partsch, K. Myers, A. Nicolaidis, and A. Cavezzi. Duplex Ultrasound Investigation of the Veins in Chronic Venous Disease of the Lower Limbs - UIP Consensus Document. Part I. Basic Principles. *Eur J Vasc Endovasc Surg*, 31:83–92, 2006.

- E. Criado, M. A. Farber, W. A. Marston, P. F. Daniel, C. B. Burnham, and B. A. Keagy. The role of air plethysmography in the diagnosis of chronic venous insufficiency. *J Vasc Surg*, 27(4):660–670, 1998.
- W. P. Donders, W. Huberts, F. N. van de Vosse, and T. Delhaas. Personalization of models with many model parameters: an efficient sensitivity analysis approach. *Int J Numer Method Biomed Eng*, 31(10):e02727, 2015.
- R. T. Eberhardt and J. D. Raffetto. Chronic Venous Insufficiency. *Circulation*, 111:2398–2409, 2005.
- V. G. Eck, W. P. Donders, J. Sturdy, J. Feinberg, T. Delhaas, L. R. Hellevik, and W. Huberts. A guide to uncertainty quantification and sensitivity analysis for cardiovascular applications. *Int J Numer Method Biomed Eng*, 32(8):e02755, 2016.
- C. J. Evans, F. G. R. Fowkes, C. V. Ruckley, and A. J. Lee. Prevalence of varicose veins and chronic venous insufficiency in men and women in the general population: Edinburgh Vein Study. *J Epidemiol Community Health*, 53(3):149–153, 1999.
- J.-M. Fullana and S. Zaleski. A branched one-dimensional model of vessel networks. *J Fluid Mech*, 621:183–204, 2008.
- W. Huberts, W. P. Donders, T. Delhaas, and F. N. van de Vosse. Applicability of the polynomial chaos expansion method for personalization of a cardiovascular pulse wave propagation model. *Int J Numer Method Biomed Eng*, 30:1679–1704, 2014.
- W. T. Jellema, B. P. M. Imholz, H. Oosting, K. H. Wesseling, and J. J. Van Lieshout. Estimation of beat-to-beat changes in stroke volume from arterial pressure: a comparison of two pressure wave analysis techniques during head-up tilt testing in young, healthy men. *Clin Auton Res*, 9:185–192, 1999.
- M. L. Katz, A. J. Comerota, and R. Kerr. Air plethysmography (APG): a new technique to evaluate patients with chronic venous insufficiency. *J Vasc Tech*, 15(1):23–27, 1991.
- J. M. T. Keijsers, C. A. D. Leguy, W. Huberts, A. J. Narracott, J. Rittweger, and F. N. van de Vosse. A 1D pulse wave propagation model of the hemodynamics of calf muscle pump function. *Int J Numer Method Biomed Eng*, 31(7):e02714, 2015.
- T. Kenner. The measurement of blood density and its meaning. *Basic Res Cardiol*, 84(2):111–124, 1989.
- T. Korakianitis and Y. Shi. Numerical simulation of cardiovascular dynamics with healthy and diseased heart valves. *J Biomech*, 39(11):1964–1982, 2006.
- W. Kroon, W. Huberts, M. Bosboom, and F. van de Vosse. A numerical method of reduced complexity for simulating vascular hemodynamics using coupled 0D lumped and 1D wave propagation models. *Comput Math Methods Med*, 2012:156094, 2012.
- N. Labropoulos, J. Tiongson, L. Pryor, A. K. Tassiopoulos, S. S. Kang, M. A. Mansour, and W. H. Baker. Definition of venous reflux in lower-extremity veins. *J Vasc Surg*, 38:793–798, 2003.
- M. H. Laughlin. Skeletal muscle blood flow capacity: role of muscle pump in exercise hyperemia. *Am J Physiol*, 253:H993–H1004, 1987.
- F. Lurie, R. L. Kistner, B. Eklof, and D. Kessler. Mechanism of venous valve closure and role of the valve in circulation: A new concept. *J Vasc Surg*, 38(5):955–961, 2003.

- E. Marchandise, M. Willemet, and V. Lacroix. A numerical hemodynamic tool for predictive vascular surgery. *Med Eng Phys*, 31:131–144, 2009.
- J. J. McCaughan, D. B. Walsh, L. P. Edgcomb, and H. E. Garrett. In vitro observations of greater saphenous vein valves during pulsatile and nonpulsatile flow and following lysis. *J Vasc Surg*, 1(2):356–361, 1984.
- G. L. Moneta, G. Bedford, K. Beach, and D. E. Strandness. Duplex ultrasound assessment of venous diameters, peak velocities, and flow patterns. *J Vasc Surg*, 8(3):286–291, 1988.
- L. O. Müller and E. F. Toro. A global multiscale mathematical model for the human circulation with emphasis on the venous system. *Int J Numer Method Biomed Eng*, 30(7):681–725, 2014.
- J. P. Mynard and J. J. Smolich. One-Dimensional Haemodynamic Modeling and Wave Dynamics in the Entire Adult Circulation. *Ann Biomed Eng*, 43(6):1443–1460, 2015.
- J. P. Mynard, M. R. Davidson, D. J. Penny, and J. J. Smolich. A simple, versatile valve model for use in lumped parameter and one-dimensional cardiovascular models. *Int J Numer Method Biomed Eng*, 28:626–641, 2012.
- A. J. Narracott, J. M. T. Keijsers, C. A. D. Leguy, W. Huberts, and F. N. van de Vosse. Fluid-structure interaction analysis of venous valve haemodynamics. In P Nithiarasu and E. Budyn, editors, *Comp Math Biomed Eng Proc*, pages 31–34, July 2015.
- A. N. Nicolaidis and A. J. Zukowski. The value of dynamic venous pressure measurements. *World J Surg*, 10:919–924, 1986.
- A.N. Nicolaidis. Investigation of Chronic Venous Insufficiency A Consensus Statement. *Circulation*, 102:e126–e163, 2000.
- S. Pant, C. Corsini, C. Baker, T. Y. Hsia, G. Pennati, and I. E. Vignon-Clementel. Data assimilation and modelling of patient-specific single-ventricle physiology with and without valve regurgitation. *J Biomech*, pages 1–12, 2015.
- J. M. Porter, G. L. Moneta, and An International Consensus Committee on Chronic Venous Disease. Reporting standards in venous disease: An update. *J Vasc Surg*, 21(4):635–645, 1995.
- B. Saltin, G. Radegran, M. D. Koskolou, and R. C. Roach. Skeletal muscle blood flow in humans and its regulation during exercise. *Acta Physiol Scand*, 162:421–436, 1998.
- A. H. Shapiro. Steady flow in collapsible tubes. *J Biomech Eng*, 99(3):126–147, 1977.
- Y. Shi, P. Lawford, and R. Hose. Review of zero-D and 1-D models of blood flow in the cardiovascular system. *Biomed Eng Online*, 10:33, 2011.
- S. Simakov, T. Gamilov, and Y. N. Soe. Computational study of blood flow in lower extremities under intense physical load. *Russ J Numer Anal M*, 28(5):485–503, 2013.
- F. N. van de Vosse and N. Stergiopulos. Pulse Wave Propagation in the Arterial Tree. *Annual Review of Fluid Mechanics*, 43(1):467–499, 2011.
- J. Werner, D. Böhringer, and M. Hexamer. Simulation and Prediction of Cardiotherapeutic Phenomena From a Pulsatile Model Coupled to the Guyton Circulatory Model. *IEEE Trans Biomed Eng*, 49(5):430–439, 2002.

- N. Westerhof and G. Elzinga. Normalized input impedance and arterial decay time over heart period are independent of animal size. *Am J Physiol*, 261(30):R126–R133, 1991.
- M. Zacek and E. Krause. Numerical simulation of the blood flow in the human cardiovascular system. *J Biomech*, 29(1):13–20, 1996.
- C. Zervides, A. J. Narracott, P. V. Lawford, and D. R. Hose. The role of venous valves in pressure shielding. *Biomed Eng Online*, 7:8, 2008.